

Limits of the time-multiplexed photon-counting method

Regina Kruse,^{1,*} Johannes Tiedau, Tim J. Bartley, Sonja Barkhofen, and Christine Silberhorn

¹*Applied Physics, University of Paderborn, Warburger Straße 100, 33098 Paderborn, Germany*

(Dated: November 15, 2016)

The progress in building large quantum states and networks requires sophisticated detection techniques to verify the desired operation. To achieve this aim, a cost and resource efficient detection method is the time-multiplexing of photonic states. This design is assumed to be efficiently scalable, however it is restricted by inevitable losses and limited detection efficiencies. Here, we investigate the scalability of time-multiplexed detectors under the effects of fibre dispersion and losses. We use the distinguishability of Fock states up to $n = 20$ after passing the time-multiplexed detector as our figure of merit and find that, for realistic setup efficiencies of $\eta = 0.85$, the optimal size for time-multiplexed detectors is 256 bins.

I. INTRODUCTION

During recent years, the progress in both quantum source [1–10] and detector [11, 12] engineering have placed the implementation of large photonic network structures into reach. However in order to verify the intended operation of the networks, reliable multi-photon measurements are necessary to both check the state generation and measure the output distribution.

One method to measure the photon number properties of a quantum state are true photon number resolving detectors, such as superconducting transition edge detectors (TES) [11]. However, while they offer intrinsic photon number resolution, they are also resource-demanding and require very low operating temperatures in the mK regime to work properly. Furthermore, their photon-number resolution is limited to a few tens of photons as the superconducting circuit breaks off at some critical energy [13–15]. Since intrinsic photon number resolving detectors have only been around recently and require a lot of resources, *quasi*-photon number resolving detectors have been proposed as a resource-efficient and cheap alternative. They use conventional on-off detectors (e.g. avalanche photo-diodes) with either a spatial or temporal multiplexing scheme [16–22]. In general, time-multiplexing can be seen as the more resource-efficient technique, as the scheme allows to use the same detectors again and again at the cost of increased measurement time, instead of using each detector only once.

The time-multiplexing network [16, 17, 19] consists of several (generally fibre-integrated) beam splitters that are connected by different fibre lengths (see fig. 1). While passing the network, one part of the input pulse is partially delayed in each beam splitter stage, such that pulses with 2^b different timings (time bins) arrive at the detector.

This method is scalable in principle, as the connection of fibre-integrated components does not pose an unsurmountable problem. In this context, Sperling et al. [23]

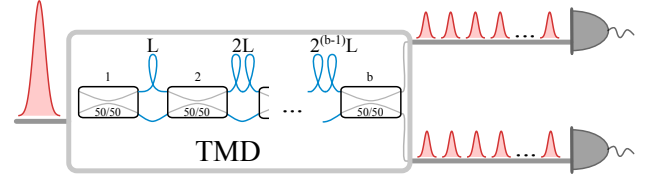


FIG. 1. (colour online) Schematic of a time-multiplexed detection network.

have considered the minimum size of a multiplexed detector to distinguish between different states in loss-free implementations. However, up to this point no investigation of the scalability has considered realistic, i.e. lossy and dispersive fibre-integrated components and their effect on the detected photon number statistics.

In this paper, we answer how scalable the time-multiplexing photon-counting detection method really is. We approach this question from an experimental point of view by simulating the photon number statistics after passing the time-multiplexing network (TMD) and compare the quality of the TMD measurement by attempting to differentiate and reconstruct different Fock state inputs. As a figure of merit, we use the overlap of the simulated photon statistics after the TMD between neighbouring Fock states and find the optimal size of the network.

The paper is structured as follows; in section II, we give a preliminary limitation of the network size, as is determined by the fibre dispersion and the input pulse length. Section III holds the discussion of the optimal network size considering state-of-the-art fibre integrated components. We discuss the effects of distributing photon-number states onto a final set of time bins and losses in the beam splitter network. Taking these two effects into account, we arrive at a practical limitation of the network size which gives the most reliable experimental data. Finally in section IV, we summarise our findings and conclude this paper.

* regina.kruse@upb.de

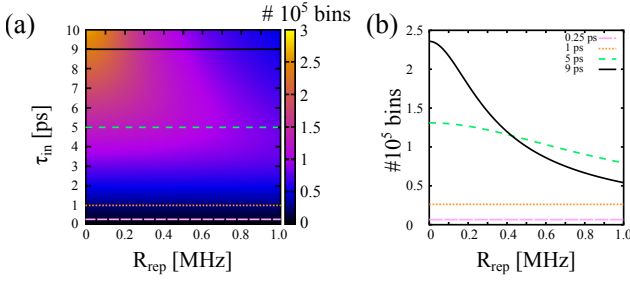


FIG. 2. (colour online) Maximum number of bins as limited by fibre dispersion. In (a) we consider the maximum time bin number depending on the repetition rate R_{Rep} and the input pulse duration. We find that even for low repetition rates and long pulse duration the number of time bins is bound by $\approx 2.5 \cdot 10^5$ bins. In (b) we cut figure (a) at fixed input pulse lengths (pink: 250 fs, orange: 1 ps, green: 5 ps and black: 9 ps). For short pulse durations the decrease in the repetition rate is compensated by the increased fibre dispersion, keeping the overall amount of time bins constant. For long pulses the dispersion is less pronounced and decreasing the repetition rate helps to increase the bin number.

II. LIMITATION VIA DISPERSION

In this section we consider the geometrical limitations of the TMD detection system, as given by the dispersion of the system. To do this, we assume no-loss fibres and detectors with unit detection efficiency and vanishing dead time. In this (admittedly unrealistic) scenario the maximum number of available bins is reached when neighbouring pulses start to overlap significantly at the output. This means that we determine this number by calculating how many output pulses fit in the time between consecutive experiments. Expressing the duration of a single shot in terms of the repetition rate of the experiment $R_{\text{rep}} = (\Delta\tau_{\text{exp}})^{-1}$, we define the maximal number of time bins as

$$N_{\text{max, disp}} = \frac{\Delta\tau_{\text{exp}}}{\Delta\tau_{\text{disp}}} = (R_{\text{rep}}\Delta\tau_{\text{disp}})^{-1}, \quad (1)$$

where $\Delta\tau_{\text{disp}}$ is the pulse width (full width at half maximum, FWHM) at the output after experiencing fibre dispersion. This effect is taken into account by the group velocity dispersion [24]

$$\Delta\tau_{\text{disp}} = \Delta\tau_{\text{in}} \sqrt{1 + \left(\frac{4 \ln(2)}{\Delta\tau_{\text{in}}^2} \cdot \frac{\lambda^2}{2\pi c} \cdot D_{\lambda} L_{\text{exp}} \right)^2}. \quad (2)$$

Here, $\Delta\tau_{\text{in}}[\text{ps}]$ is the FWHM pulse length of the input photons, $\lambda = 1550 \text{ nm}$ the operating wavelength, D_{λ} the dispersion coefficient and $\Delta\tau_{\text{disp}}[\text{ps}]$ the output pulse length after passing a fibre of length $L_{\text{exp}} = c \cdot \Delta\tau_{\text{exp}}[\text{km}]$ with c as the speed of light in the fibre. The dispersion coefficient D_{λ} for standard SMF28 fibres is specified with $D_{\lambda} \leq 18.0 \frac{\text{ps}}{\text{nm} \cdot \text{km}}$ [25] at 1550 nm.

As (2) applies to the FWHM of the output pulses, we have artificially halved the number of available time bins

from equation (1) to guarantee that the different time bins can be resolved in the experiment. The results are given in figure 2. In figure 2(a), we plot the maximum number of available time bins depending on the repetition rate of the experiment, as well as on the input pulse duration which undergoes fibre dispersion. We consider only repetition rates below 1 MHz, as they give sufficient time between two experiments, while still allowing for sufficient data rates. Even for low repetition rates (long time between two consecutive experiments) and long input pulses (low dispersion effect) we find that the maximum number of time bins is bounded by approximately $2.5 \cdot 10^5$ bins. Figure 2(b) examines the effect of dispersion in more detail. We cut through panel (a) at specified input pulse lengths of 250 fs in pink, 1 ps in orange, 5 ps in green and 9 ps in black. It becomes clear that for short pulse durations the longer timescale between experiments at low repetition rates is fully compensated by the increased fibre dispersion and the number of available time bins remains approximately constant.

For longer input pulses, the dispersion plays a smaller role, which is why we cut the plot at $\tau_{\text{in,max}} = 10 \text{ ps}$. The number of available time bins is accordingly higher and increases even for smaller repetition rates, as the fibre dispersion is not strong enough to eliminate the advantage of longer times between experiments.

From this result, we can conclude the hard limit of available time bins in fibre-integrated TMD systems due to dispersion. For short input pulses, the available number of bins is rather limited while longer pulses allow for quite high photon number resolution. However, up to this point we have not considered losses in the system which will deteriorate the detected photon number statistics (click statistics) of the input state.

III. LIMITATION VIA LOSS

In the previous section, we have considered an ideal fibre integrated system without loss and perfect detectors. Now, we consider a system including losses and finite setup transmission and detection efficiency. We will investigate the ability to discriminate between different Fock states from their measured photon number statistics and will also comment on the reconstruction limitations of Fock states by scanning the overlap of the adjacent Fock states and using the width of this curve as a measure for the reconstruction error.

A. Model and Parameters

The action of the TMD on photon number statistics is governed by two mechanisms: the convolution matrix that describes the distribution of n photons on a finite number of N bins [19] and losses that directly deteriorate the photon number statistics.

For this work, we use the photon counting formula as proposed by Sperling et al. [23]. As their model only accounts for perfect 50/50 beam splitters in the TMD (i.e. perfectly even photon distribution among the bins), this formula will only be an approximation of the expected photon number statistics in an experiment. However, as we are only interested in limitations of the measurement method this approximation is justified. With the photon counting formula, we can formulate the convolution matrix C

$$C_{n',k} = \begin{cases} \frac{1}{N^{n'}} \binom{N}{k} \sum_{j=0}^k (-1)^j \binom{k}{j} (k-j)^{n'}, & \text{if } n' \geq k \\ 0, & \text{else} \end{cases} \quad (3)$$

that gives the probability of measuring k clicks when n' photons impinge on N detectors (in our case $N = 2^b$ time bins). For more details see [23].

The second mechanism is the impact of loss on the photon number statistics. The expression for the loss matrix is well-known and given by e.g. [19]

$$L_{n,n'} = \binom{n}{n'} \eta^{n'} (1-\eta)^{n-n'}. \quad (4)$$

It describes the probability of retaining n' photons out of n with a finite efficiency η . In our case, the losses are defined by the number of beam splitters, the longest fibre length that the photons have to pass, as well as non-unit detection efficiencies.

Finally, the resulting click distribution after passing the TMD is given by [19]

$$p_k^{(\text{out})} = C_{n',k} L_{n,n'} \rho_n^{(\text{in})}. \quad (5)$$

To simplify our investigation, we will consider loss and convolution as separate processes. We assume that the convolution is governed by perfect 50/50 beam splitters in the TMD, while loss effects the click statistics separately. This assumption will only provide an approximation of the realistic click statistics as losses inside the fibre network or non-perfect detection efficiencies modify the splitting ratio of the beam splitter network [19].

For experimental parameters, we consider freely available, state-of-the-art fibre-integrated components. We assume that our detectors offer a dead time 10 ns, which might be achievable for superconducting nanowire detectors in the future [26]. Furthermore, we assume fibre losses of $0.2 \frac{\text{dB}}{\text{km}}$ [25] and a minimal loss of 0.05 dB per beam splitter [27]. We will neglect the losses of the fibre splices, as they are very low compared to the splitter and fibre loss. If not specified otherwise, we assume perfect setup transmission (prior to the TMD) and detection efficiency η_{ex} .

B. Photon Number Discrimination

In the following, we consider pure Fock states as test cases for our TMD investigation. They have the advantage

that they are orthonormal in the input and that the effect of modified click statistics is most pronounced.

To quantify the effect of TMD measurements on the input statistics, we first consider the effects of the convolution and loss separately in figure 3(a). In black, we have plotted the overlap of the click statistics of the two Fock states $\langle 15 | 20 \rangle$ as an example. As expected [23], the overlap decreases to higher bin numbers as the effect of the convolution decreases and the click statistics approximate the true photon number statistics. The opposite is true for the losses, as shown in blue. As the number of beam splitters and fibre length increases, so do the losses for more bins. Accordingly, the click statistics are washed out and the overlap increases. Therefore when considering both convolution and loss effects (plotted in red), we find an optimal bin number where the overlap between the two Fock states after passing the TMD is minimal.

In figures 3(b)-(d), we have extracted the optimal TMD parameters for different input Fock states and detection efficiencies. We consider neighbouring (black) Fock states, next-nearest neighbours (blue) and states with four numbers in between (green). We find that even for the ideal case of perfect setup transmission and detection efficiency in figure 3(b), the optimal bin number for all three cases at high photon numbers does not exceed 256 bins. The associated overlap for the optimal bin numbers (plotted as inlays) is a monotonically increasing function of the photon number and reaches one asymptotically. Realistically, this curve will have to be truncated at a critical overlap value that depends on the application, the robustness of the reconstruction algorithm of choice and also on the tolerable measurement time and statistical errors in the experiment.

Adding loss that accounts for imperfect setup transmission and detection efficiency in figures 3(c) and (d) deteriorates the click statistics quite drastically. In this case, the optimum bin numbers are lower than for the ideal case, while the overlap curves approach one faster. In the case of a realistic, overall experiment efficiency of $\eta_{\text{ex}} = 0.85$, it becomes clear that for our figure of merit the optimal TMD size does not exceed $256 = 2^8$ bins.

C. Photon Number Reconstruction

In the last section, we have seen that it does not have an advantage to build TMDs bigger than 256 time bins, when using the setup to discriminate between Fock states. However, this might not be the only aim of a quasi-photon number resolved detection. Another significant task is to reconstruct the impinging states on the TMD. To this aim a lot of reconstruction algorithms have been proposed and implemented (e.g. see [28–30]). In this paper, we do not want to comment on the advantages or disadvantages of the particular reconstruction methods and only want to infer an error bar from the measured statistics that will affect the precision of the

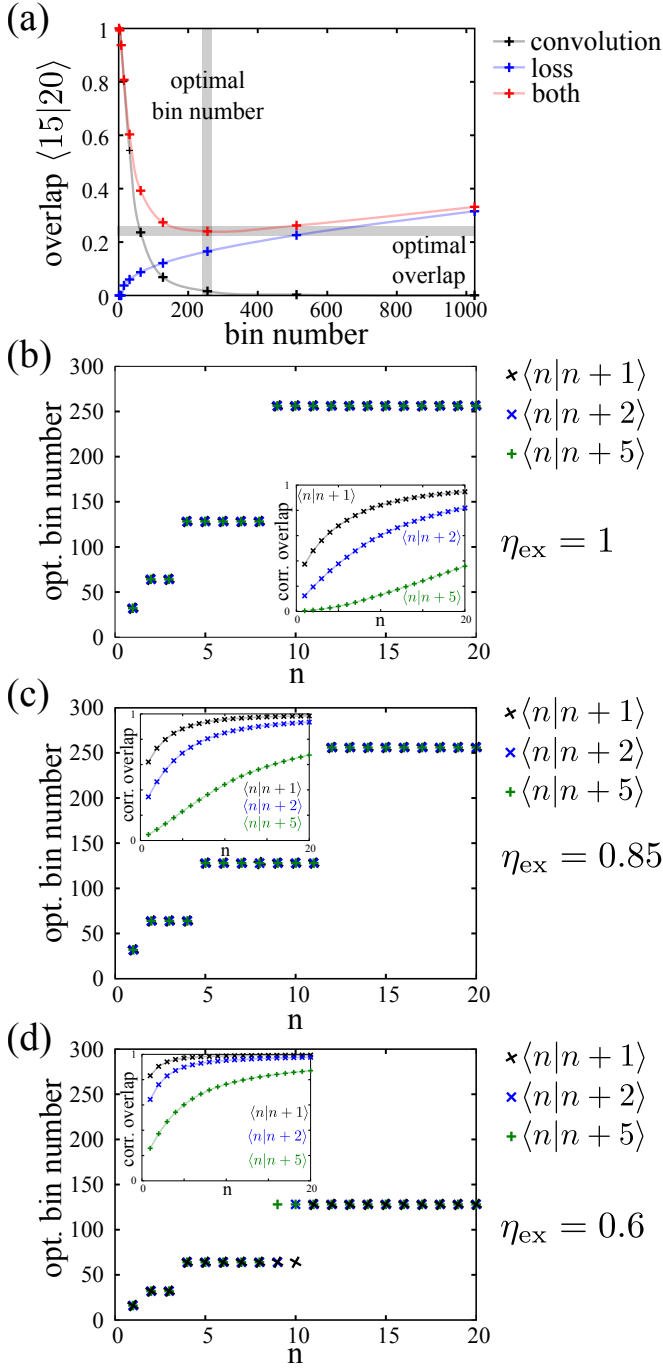


FIG. 3. (colour online) Overlap of the click statistics between different Fock states after passing a TMD. In (a) we consider the different contributions to the final overlap separately for the example $\langle 15|20 \rangle$. For small bin numbers, the overlap is governed by the convolution matrix (black), for high bin numbers by the losses (blue). The minimum of the curve that considers both effects (red) gives the optimal parameters for minimal overlap, marked in grey. In figures (b)-(d), we have extracted the optimal bin number and overlap (curves in the inlays) for different detection and setup efficiencies η . The additional losses deteriorate the click statistics quite severely, such that for realistic setup and detection efficiencies ($\eta = 0.8$) it holds no advantage to implement larger than 256-bin TMDs. The faint lines hold no physical meaning and are provided as a guide to the eye.

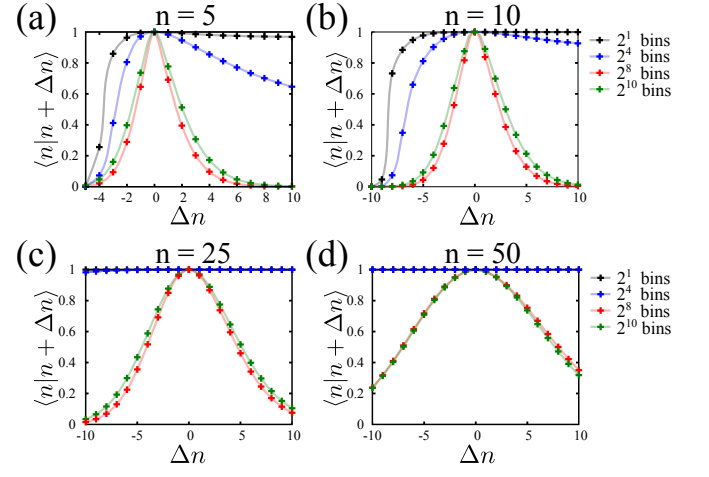


FIG. 4. (colour online) For different, but fixed Fock state inputs $|n\rangle$, we calculate the overlap to the adjacent ± 10 Fock states in the click statistics after passing TMDs of different size. The width of the overlap curve gives a measure with which precision a Fock state can be measured and is therefore a criterion for the resolution of the measurement method. Even for very small input Fock states ($n = 5$ in (a)) large TMDs (2¹⁰ bins in green) do not perfectly resolve the input state. For larger states (e.g. $n = 50$ in (d)), the resolution goes down drastically. From this we conclude that TMDs are not sufficient to verify large quantum states directly. The faint lines in the figures hold no physical meaning and are provided as a guide to the eye.

reconstruction.

To this aim, we regard a pure Fock state $|n\rangle$ impinging on our detector without excess loss ($\eta_{\text{ex}} = 1$) and calculate the overlap of the click statistics after the TMD for the 20 adjacent Fock states $\langle n-10|n \rangle$ to $\langle n|n+10 \rangle$. The results for different input states $|n\rangle$ and different bin numbers are depicted in figure 4.

As an example, let us consider figure 4(a). We have colour-coded the overlap of the click statistics after passing TMDs of different sizes. Consider the red curve for passing a 256-bin TMD. The curve peaks at $\Delta n = 0$, as we send the same state into the TMD. It is slightly asymmetric with respect to $\Delta n = 0$, as the binomial coefficients that govern the overlap of the click statistics are different for the higher and lower photon number cases. This effect evens out to higher input Fock states (compare 4(d)) as the relative difference in the input photon number decreases.

As we increase the photon number of the input Fock states, the overlap curve between the click statistics becomes broader for all considered TMD sizes. This is expected due to the increased impact of the convolution matrix for higher photon numbers. However, it also becomes clear that the improvement of larger TMDs for large input states is not very pronounced. Especially for figure 4(d) the improvement in the width of the overlap curve between 256 and 1024 bins does not really justify the experimental effort it takes to fabricate a high qual-

ity TMD of that size. Furthermore, one has to consider the impact of finite detection efficiencies and setup transmission. We have seen in the previous section that the increased losses only deteriorate the statistics further and render building large TMDs without a real advantage.

IV. CONCLUSION

In conclusion we have investigated the limitations of photon number resolved measurements by time-multiplexed detection (TMDs). We have discussed the fundamental limit of the device as given by its dispersive fibre-integrated design. Furthermore, we have considered the combined effect of losses and convolution in the con-

text of photon number discrimination tasks, as well as for photon number state reconstruction. Both cases show that building large TMDs is not advantageous since losses deteriorate the photon number statistics faster than the effect of the convolution matrix diminishes. As a recommendation based on realistic experimental figures of merit, we suggest using 256 bin devices, as they provide both moderate losses and moderate photon number resolution.

Acknowledgements

The authors would like to thank Martin Bohmann for valuable discussions concerning the photon counting formula. This work was supported by the European Union Grant No. 665148 (QCUMbER). T. J. Bartley acknowledges support from SFB/TRR 142.

-
- [1] P. J. Mosley, J. S. Lundeen, B. J. Smith, P. Wasylczyk, A. B. U'Ren, C. Silberhorn, and I. A. Walmsley, *Physical Review Letters* **100**, 133601 (2008).
 - [2] A. Eckstein, A. Christ, P. J. Mosley, and C. Silberhorn, *Physical Review Letters* **106**, 013603 (2011).
 - [3] G. Harder, V. Ansari, B. Brecht, T. Dirmeier, C. Marquardt, and C. Silberhorn, *Optics Express* **21**, 13975 (2013).
 - [4] M. J. Collins, C. Xiong, I. H. Rey, T. D. Vo, J. He, S. Shahnia, C. Reardon, T. F. Krauss, M. J. Steel, A. S. Clark, and B. J. Eggleton, *Nature Communications* **4**, 2582 (2013).
 - [5] R. Kumar, J. R. Ong, M. Savanier, and S. Mookherjee, *Nature Communications* **5**, 5489 (2014).
 - [6] N. Bruno, A. Martin, T. Guerreiro, B. Sanguinetti, and R. T. Thew, *Optics Express* **22**, 17246 (2014).
 - [7] R.-B. Jin, M. Fujiwara, T. Yamashita, S. Miki, H. Terai, Z. Wang, K. Wakui, R. Shimizu, and M. Sasaki, *Optics Communications* **336**, 47 (2015).
 - [8] M. Förtsch, G. Schunk, J. U. Fürst, D. Strekalov, T. Gerrits, M. J. Stevens, F. Sedlmeir, H. G. L. Schwefel, S. W. Nam, G. Leuchs, and C. Marquardt, *Physical Review A* **91**, 023812 (2015).
 - [9] K. Zielnicki, K. Garay-Palmett, R. Dirks, A. B. U'Ren, and P. G. Kwiat, *Optics Express* **23**, 7894 (2015).
 - [10] G. Harder, T. J. Bartley, A. E. Lita, S. W. Nam, T. Gerrits, and C. Silberhorn, *Physical Review Letters* **116**, 143601 (2016).
 - [11] A. E. Lita, A. J. Miller, and S. W. Nam, *Optics Express* **16**, 3032 (2008).
 - [12] F. Marsili, V. B. Verma, J. A. Stern, S. Harrington, A. E. Lita, T. Gerrits, I. Vayshenker, B. Baek, M. D. Shaw, R. P. Mirin, and S. W. Nam, *Nature Photonics* **7**, 210 (2013).
 - [13] D. Fukuda, G. Fujii, T. Numata, K. Amemiya, A. Yoshizawa, H. Tsuchida, H. Fujino, H. Ishii, T. Itatani, S. Inoue, and T. Zama, *Optics Express* **19**, 870 (2011).
 - [14] T. Gerrits, B. Calkins, N. Tomlin, A. E. Lita, A. Migdall, R. Mirin, and S. W. Nam, *Optics Express* **20**, 23798 (2012).
 - [15] P. C. Humphreys, B. J. Metcalf, T. Gerrits, T. Hiemstra, A. E. Lita, J. Nunn, S. W. Nam, A. Datta, W. S. Kolthammer, and I. A. Walmsley, *New Journal of Physics* **17**, 103044 (2015).
 - [16] D. Achilles, C. Silberhorn, C. Śliwa, K. Banaszek, and I. A. Walmsley, *Optics Letters* **28**, 2387 (2003).
 - [17] J. Řeháček, Z. Hradil, O. Haderka, J. Peřina, and M. Hamar, *Physical Review A* **67**, 061801 (2003).
 - [18] M. J. Fitch, B. C. Jacobs, T. B. Pittman, and J. D. Franson, *Physical Review A* **68**, 043814 (2003).
 - [19] D. Achilles, C. Silberhorn, C. Sliwa, K. Banaszek, I. A. Walmsley, M. J. Fitch, B. C. Jacobs, T. B. Pittman, and J. D. Franson, *Journal of Modern Optics* **51**, 1499 (2004).
 - [20] E. Waks, E. Diamanti, B. C. Sanders, S. D. Bartlett, and Y. Yamamoto, *Physical Review Letters* **92**, 113602 (2004).
 - [21] L. A. Jiang, E. A. Dauler, and J. T. Chang, *Physical Review A* **75**, 062325 (2007).
 - [22] R. Heilmann, J. Sperling, A. Perez-Leija, M. Gräfe, M. Heinrich, S. Nolte, W. Vogel, and A. Szameit, *Scientific Reports* **6**, 19489 (2016).
 - [23] J. Sperling, W. Vogel, and G. S. Agarwal, *Physical Review A* **85**, 023820 (2012).
 - [24] J.-C. Diels and W. Rudolph, *Ultrashort Laser Pulse Phenomena*, Second Edition, 2nd ed., edited by P. F. Liao and P. Kelley (Academic Press, Amsterdam ; Boston, 2006).
 - [25] Corning Optical Fibre, "Optical Specifications of SMF28e fibres," (2007).
 - [26] A. J. Annunziata, O. Quaranta, D. F. Santavica, A. Casaburi, L. Frunzio, M. Ejrnaes, M. J. Rooks, R. Cristiano, S. Pagano, A. Frydman, and D. E. Prober, *Journal of Applied Physics* **108**, 084507 (2010).
 - [27] Evanescent Optics Inc., "Low loss in fibre-integrated beam splitters," private communication (2016).
 - [28] G. Zambra, A. Andreoni, M. Bondani, M. Gramegna, M. Genovese, G. Brida, A. Rossi, and M. G. A. Paris, *Physical Review Letters* **95**, 063602 (2005).
 - [29] A. V. Dodonov, S. S. Mizrahi, and V. V. Dodonov, *Physical Review A* **74**, 033823 (2006).
 - [30] A. Allevi, M. Bondani, and A. Andreoni, *Optics Letters* **35**, 1707 (2010).